Clinical Neurophysiology 130 (2019) 396–405

Contents lists available at ScienceDirect

Clinical Neurophysiology

journal homepage: www.elsevier.com/locate/clinph

Similarities and differences between the interictal epileptiform discharges of green-spikes and red-spikes zones of human neocortex

Ruggero Serafini *

Department of Neurology, University of Utah, Clinical Neuroscience Center, George E. Wahlen VA Medical Center, Salt Lake City, UT, USA

ARTICLE INFO

Article history:
Accepted 19 December 2018
Available online 19 January 2019

Keywords:
Neocortical epilepsy
Spike-and-slow-wave complexes
Surround inhibition
Green-spikes and red-spikes zones

HIGHLIGHTS

- In intracranial EEGs, interictal discharges differ between green- and red-spikes zones.
- Interictal discharges slow-waves at the edge of a focus may reflect surround inhibition.
- Slow-waves persist at the edge of green-spikes zones but decrease at the edge of red-spikes zones.

ABSTRACT

Objective: This study looks for differences in the waveforms of interictal epileptiform discharges (IEDs) between cortices expressing only isolated discharges (green-spikes zones) vs those manifesting seizures (red-spikes zones): these can help to understand ictogenesis mechanisms and improve clinical decision in surgical epilepsy. Typical IEDs are triphasic, exhibiting in sequence: a negative-sharp-wave, a positive-baseline-shift and a negative-slow-wave. Negative-slow-waves are thought to reflect neurophysiological inhibition: their features at a focus' edge may reflect *peripheral* inhibition, a mechanism characterized in experimental models, curbing seizures' spread. This might be weakened in red-spikes.
Methods: A retrospective review of human intracranial EEGs was performed, comparing green- and red-spikes for their peripheral slow-waves' amplitudes. Green- and red-spikes were also compared also for the amplitudes of their negative-sharp-waves and positive-baseline-shifts, as well as for their spread pathways.
Results: Green-spikes exhibit more pronounced peripheral slow-waves than red-spikes. They also exhibit more pronounced positive-baseline-shifts, and more frequent propagation pathways' shifts.
Conclusions: Peripheral slow-waves' amplitudes *correlate with* seizures' suppression and may reflect neurophysiological peripheral inhibition.
Significance: This study suggests a novel approach to reading intracranial EEGs: amplitudes measures of IEDs waveforms are technically simple, may help identifying epileptogenic zones and indicate the spatial distribution of underlying ictogenesis mechanisms.

1. Introduction

This project studies the waveforms of interictal epileptiform discharges (IEDs) recorded in human intracranial EEGs. It attempts to identify features specific of cortices generating only interictal discharges (green-spikes zones) and of those generating not only interictal discharges but also seizures (red-spikes zones): these could yield insight into ictogenesis mechanisms and also be used as a biomarker to improve clinical decision making in surgical epilepsy.

About 30% of epilepsy patients suffer from intractable drug-resistant seizures. Surgical resection cannot always improve the control of seizures, because identifying the cortical regions that generate seizures can be difficult, (Jehi, 2008) especially with neocortical epilepsy (Noe et al., 2013). Improving our understanding of epilepsy neurophysiology can facilitate the development of novel diagnostic and therapeutic options.

Epileptic foci may generate sporadic, isolated, spatially confined discharges (IEDs), but in seizures they also produce a different modality of activity with spreading rhythmic repetitive waves. Experimental models of epilepsy showed that the occurrence of

* At: Department of Neurology, University of Utah, Clinical Neuroscience Center, 175 North Medical Drive East, 5th floor, Salt Lake City, UT 84132, USA.
E-mail address: ruggero.serafini@yahoo.com

https://doi.org/10.1016/j.clinph.2018.12.011
1388-2457/

seizures is regulated by an inhibitory mechanism (Trevelyan and Schevon, 2012) at the periphery of a cortical discharge zone (Prince and Wilder, 1967).

Identifying zones generating seizures can guide selective resections and yield insight into epilepsy neurobiology. Epileptologists have long but unsuccessfully searched for EEG features specific of interictal epileptiform discharges in zones generating seizures (red-spikes zones) vs those in zones generating only IEDs (green-spikes zones) (Luders et al., 2006; Palmini, 2006). Indeed, to the knowledge of this writer, the very terms green-spikes vs red-spikes are not utilized in current clinical electroencephalography practice.

Clues to identify the red-spikes zone may come from the waveforms of epileptic discharges. Typical IEDs are triphasic, exhibiting a sequence of a negativesharp-wave, a positive-baseline-shift and a negative-slow-wave. The initial negative sharp waves correlate with a paroxysmal depolarization shift and increased action potential firing. The latter are followed by a prolonged hyperpolarization with inhibition of the firing rate (Matsumoto and Ajmone-Marsan, 1964; Dichter and Spenser, 1969a, 1969b; Babb and Crandall, 1976; Buzsaki, 1986). The slow-wave recorded in surface electrodes correlates in time with and reflects such inhibitory hyperpolarization (Pollen, 1964; discussed in Engel, 1990).

Thus, characterizing waveform features of EEG sharp-waves and slow-waves across the surface of an epileptic focus may offer insight on the spatial distribution of underlying neuronal generators, both excitatory and inhibitory.

In a previous study (Serafini and Loeb, 2015), we showed that the amplitudes of sharp-waves and slow-waves of human intracranial EEGs varied across the surface of epileptic foci: discharges at the center exhibited a prevalent sharp-wave while those at the periphery exhibited a relative enhancement of the slow-wave. As slow-waves are known to correlate with and reflect inhibition, we inferred that their peripheral increase in amplitude might possibly correspond to the surround inhibition described in experimental epilepsy models.

In this study, I tested whether the features of sharp-waves and slow-waves across the discharge zone may reveal differences distinguishing green-spikes from red-spikes zones. I show that in subdural grids recordings from 22 consecutive patients, peripheral slow-waves' relative increase in amplitude is pronounced in green-spike zones but lost in red-spikes zones: peripheral slow-waves' relative increase in amplitude, therefore, correlates with inhibition of epileptiform spread. This finding corroborates the hypothesis that peripheral slow-wave may correspond to an inhibitory mechanism.

The measurements of intracranial EEG IEDs waveforms, that I am proposing, are technically simple so as to be easily implemented in clinical practice and can be valuable to map the spatial distribution of ictogenesis mechanisms as well as to indicate cortical areas that generate seizures.

2. Subjects/materials and methods

Intracranial EEG recordings were reviewed and analyzed as previously described (Serafini and Loeb, 2015). In this study I performed the same type of data analysis on the recordings from another database of intracranial EEG recordings.

2.1. Inclusion and exclusion criteria

I reviewed the database of the comprehensive epilepsy program of the University of Utah, and looked for the intracranial EEGs performed between 2012 and 2016. Of the recordings performed within this time interval, 36 patients' consecutive cases were available.

The inclusion criteria were identical to the previous study, namely, the presence of interictal epileptiform discharges (IEDs) in subdural grids and/or strips, regardless of age, sex, race, ethnicity, frequency of seizures, and pharmacological treatment.

Exclusion criteria and rationale of the exclusion were as follows. (1) IEDs only in depth electrodes but not in subdural grids were excluded because in these the spatial distribution over the neocortex could not be determined. (2) IEDs with the electrode exhibiting the highest voltage sharp wave at an edge electrode of the strip were excluded because in these, it was difficult to assess the electrodes' location relative to the spatial extension of the focus, whether at the center or at the very periphery. (3) IEDs which did not exhibit a sharp-and-slow-wave electrographic morphology (such as for example, polyspikes not followed by a slow-wave) were not included because in these the peripheral enhancement/persistence of the slow-wave could not be determined. Four cases were excluded because of (1); four cases because of (2); and six cases because of (3). The analysis was performed on all the remaining 22 consecutive cases.

2.2. Intracranial EEG recordings

Recordings had been performed through electrodes manufactured by AD-TECH Medical Instruments (WI). Inter-electrode distance was of 10 mm. Data were in two different digital data formats, in Compumedics-Nexus and Natus-Neuroworks, respectively.

The 22 cases utilized for this study (Table 1) were divided into three groups:

(1) Patients whose intracranial recordings exhibited discharge zones with only interictal discharges but no seizures (green-spikes). In this group of patients, seizures were recorded, too, but they manifested in electrodes different from those exhibiting only isolated discharges. In 5/6 of these cases, seizures electrodes were located on 1×4 or 1×6 electrodes strips in subtemporal or mesial temporal location while green spikes electrodes were on grids over the neocortex. In 1/6 of these, seizures electrodes did not show interictal discharges. In the remaining 5/6 of these, seizure electrodes exhibited also isolated discharges but the highest voltage sharp-wave was at the edge electrode of the strip (see previous section on inclusion and exclusion criteria).
(2) Patients whose intracranial recordings exhibited both foci with isolated discharges without seizures (green-spikes zone) and foci with both isolated discharges and seizures (red-spikes zones). Differently from the cases of group 1, zones with seizures of group 2 met the inclusion criteria for data analysis.
(3) Patients whose intracranial recordings exhibited only foci with both isolated discharges and seizures (red-spikes zones).

In recordings of green-spikes zone from ten patients, discharges were captured by an 8×8 grids in n = 7 patients; by an 8×4 grid in n = 1; and only in n = 2 the electrodes belonged to a linear strip of 1×6 electrodes. In recordings of the red-spikes zones from sixteen patients, in n = 5 cases discharges belonged to a linear strip (1×8 or 1×6 or 1×4 strips), while in the other n = 9 cases they belonged to 8×8 grids.

Discharges utilized for this study exhibited a high signal-to-noise ratio (waveforms of hundreds of microvolts vs baseline noise of ~50 microvolts) and an electrographic morphology typical of

Table 1
Demographics, anatomy, pathology, outcomes and number of discharge zones.

#	Gender	Age at surgery	Years with sz	Lobe	Pathology	Engel class outcomes	No. IED zones	No. Sz zones
Zones without seizures								
1	F	29	9	Frontal	No resection	–	1	–
2	F	46	37	Temporal	gliosis	I	1	–
3	M	23	19	Temporal	MTS and gliosis	I	1	–
4	M	23	2	Frontal	CD 2 A	I	1	–
5	F	25	17	Temporal	Neuronal loss	III	1	–
6	M	30	11	Temporal	CD 2A	I	2	–
Zones with and zones without seizures								
7	F	16	7	Frontal	No resection	–	1	1
8	F	50	14	Temporal	No resection	–	1	1
9	F	40	31	Frontal	No resection	–	1	1
Zones with seizures								
10	F	31	10	Parietal	DNET	I	–	1
11	F	47	47	Temporal	Gliosis + MTS	I	–	1
12	F	34	30	Frontal	CD IIB + gliosis	II	–	1
13	F	22	7	Temporal	No resection	–	–	1
14	F	27	24	Frontal	CD 2A	II	–	1
15	M	32	21	Parietal	CD 2B	I	–	1
16	M	47	5	Frontal	No resection; Hx Meningioma	–	–	1
17	F	25	12	Cingulate	No resection	–	–	1
18	F	30	29	Temporal	No resection	–	–	1
19	F	59	42	Temporal	CD 1A	IV	–	1
20	M	27	21	Temporal	MTS?	I	–	1
21	F	19	5	Parietal	CD 2B	I	–	1
22	M	43	26	Temporal	No resection	–	–	1

Abbreviations. IEDs: Interictal epileptiform discharges. MTS: mesial temporal sclerosis. CD: cortical dysplasia. Hx: history of. DNET: dysembryoblastic neuroepithelial tumor. No. IED zones and No. sz zones: number of zones that have been used for the measurements of this study, for the green-spikes and red-spikes zones, respectively.
Engel Class Outcomes refers to the scale of outcomes after epilepsy surgery. Class I: Free of disabling seizures. Class II: Rare disabling seizures. Class III: Worthwhile improvement. Class IV: No worthwhile improvement.

interictal epileptiform discharges, allowing for an easy and unequivocal detection. The identification of interictal discharges and of seizures was performed independently by two physiologists, each of the Attending Epileptogists responsible of the clinical management of each patient and subsequently the author of this study. The duration of the recordings available for the review and actually reviewed was of 772 ± 159 min (μ + SE). The median was 453 min and the range was 98–3120 min.

The discharges utilized for the study were representative of each discharge zone and were consistent throughout each recording. For the data in Compumedics-Nexus format, I obtained averages of the waveforms for the channels exhibiting discharges, using at least 5 consecutive discharges. For data in the Natus-Neuroworks format, I reviewed data and performed measurements of multiple consecutive discharges and calculated the corresponding averages. Upon a comparison between the values of the two data sets and related approaches, differences between them were of less than 30% and were neither relevant nor statistically significant: the differences between green-spike and red-spike zones we present in this study were evident in each of the data-sets.

2.3. Operational definition of the center and the periphery of the discharge zone

The typical IED waveforms exhibit multiple phases. The most common ones in due sequence are: a sharp-wave, a positive (downward) baseline-shift and a slow-wave (Chang et al., 2011). The sharp-wave is occasionally preceded by a low voltage, positive polarity component, and in this study I am naming it as the positive prepotential. I also noticed an additional waveform component, a low voltage, negative polarity wave at the onset of the discharge (a *negative* prepotentail) preceding the positive prepotential (see Fig. 1A).

The sharp-wave has usually its highest voltage in one or more electrodes. In the surrounding electrodes, its voltage gradually declines as a function of distance, until it disappears into the baseline activity at the edges of the discharge zone. The electrode with the highest amplitude sharp-wave is termed as the "center" of the discharge zone. The adjacent electrodes are termed the "surround" or "periphery". Details and illustration on the classification/distinction of electrodes between center and periphery can be seen also in Fig. 1 of a previous study (Serafini and Loeb, 2015).

2.4. Rationale and methodology of comparing center vs periphery

I plotted the amplitudes of sharp-waves and of slow-waves in the surround electrodes as a function of their distance from the center. Despite location-dependent variations of discharge amplitude, waveform analysis can still reveal localized enhancement of inhibition. Comparing amplitudes of slow-waves and sharp-waves and calculating their ratios may disclose local relative enhancement, invariance or loss of the slow-wave. The ratio of slow-wave/sharp-wave should reflect ratios of corresponding cellular/synaptic generators.

Thus, in the channel corresponding to each electrode, I measured the amplitudes of sharp- and slow-waves and then I calculated the ratios of slow-wave/sharp-wave as a function of their distance from the highest sharp-wave electrode. I assessed for consistency of these values throughout each recording. Then, I organized distance values in zones corresponding to: 1–2, 2–3 and 3–4 cm. I limited statistical comparisons to waveforms at 1–2 cm and 2–3 cm zones, because discharges from the 3–4 cm and above can be observed in only few recordings, have low amplitude, and their measurements are less accurate. Reported values are averages for bins corresponding to the above described zones (see Fig. 1B and D).

2.5. Experimental design: primary and secondary endpoints

I compared the measured values of the green-spike zones vs the corresponding ones of the red-spike zone.

Primary measurement endpoints were: (i) amplitudes of the sharp-waves, (ii) amplitudes of the slow-waves and, (iii) ratios of ii/i, that is, of slow-wave/sharp-waves. These were measured at the center of the discharge and, in the surrounding electrodes where discharges exhibited a defined sharp-and-slow-wave morphology.

To cover systematically all components of epileptiform discharges waveforms, as secondary end-points I also measured: (i) amplitudes of the positive-baseline-shift between sharp-wave and slow-wave; (ii) amplitudes of the positive pre-potentials. Additional secondary endpoints were: (iii) kinetics of discharges; (iv) spatial spread area, (v) lead electrode commencing the discharges and subsequent propagation path.

To perform statistical comparisons between the values of the green-spikes zone vs the corresponding ones of the red-spikes zone, I utilized a commercial spreadsheet software (Kaleidagraph, Reading, PA, USA). Wilcoxon test was preferred so as to allow statistical comparisons of data after normalization and/or not nor-

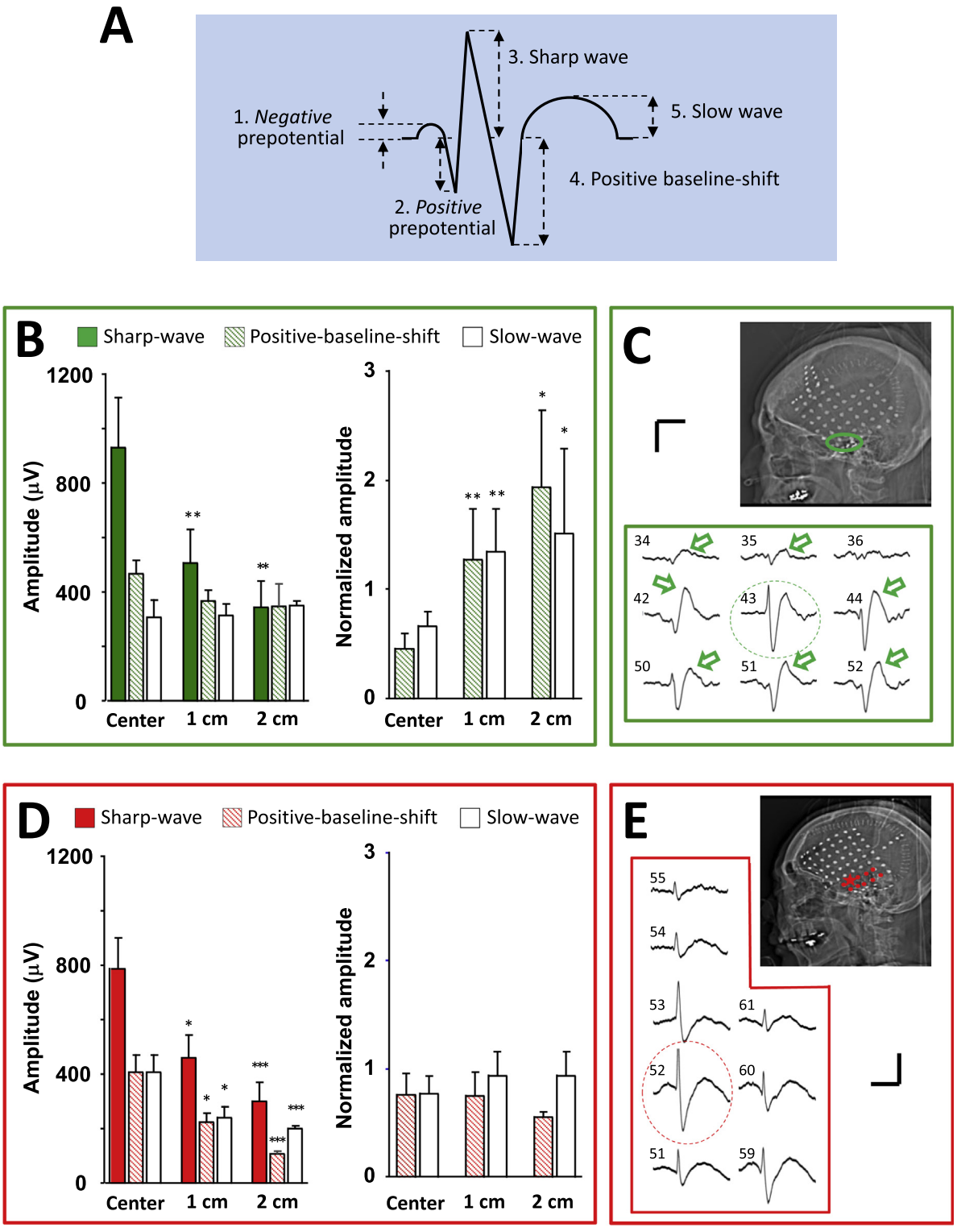

mally distributed. For statistical analysis of frequencies (see Tables 2 and 3) I performed Fisher's exact test through an online version of GraphPad (https://www.graphpad.com/quickcalcs/contingency1.cfm). A priori statistical significance value was $p < 0.05$.

The review of the recordings and waveforms' measurements were performed by the author in blind, without knowing the demographics, or the clinical history of the patients and without knowing whether interictal discharges belonged to green-spikes or red-spikes zones. Classification into green-spikes and red-spikes zones groups was obtained only after the measurements were performed.

3. Results

3.1. Peripheral slow-wave enhancement is attenuated in the red-spikes zones: general overview and hypothesis generation

A previous study (Serafini and Loeb, 2015) showed that the ratio of amplitudes of slow-wave/sharp-wave varies sizably not only within various areas of the same epileptic focus but also between different epileptic foci. We entertained the hypothesis that there could be two classes of epileptic foci: (i) foci with a pronounced change of the waveform morphology between center and periphery and (ii) foci in which waveforms showed small differences between center and periphery.

Slow-waves are thought to reflect inhibition: thus, the relative enhancement of peripheral slow-waves might possibly correspond to the surround inhibition described in experimental epilepsy models. This hypothesis would predict that in red-spikes zones, the relative enhancement of peripheral slow-wave would be weaker: so seizures' occurrence would correlate with lower peripheral slow-waves. I have tested this hypothesis in a different database and with a larger sample size.

3.2. Primary end-points: the relative-enhancement of peripheral slow-waves is attenuated in red-spikes zones

Averaging data from multiple recordings, at the center, the amplitudes of the sharp-wave and of the slow-wave were similar (Fig. 1B and D) between green-spikes and red-spikes zones.

At 1 cm away from the center, the sharp-wave amplitude decreases by ~45% in both the green spikes and the red spikes zones (filled bars of the histograms on the left). The space-dependent slow-wave change is different between green-spikes and red-spikes zones (empty bars of the histograms on the left): it increases slightly (~1.3 fold) in green-spikes zones, but it decreases by 25% in red-spikes zones. The relative amplitude of slow-wave vs the sharp-wave as measured by the slow-wave/sharp-wave ratio at different distances from the center does not change in red-spikes zones, while it doubles in red-spikes zones (empty bars of the histograms on the right). This space-dependent pattern becomes more pronounced at 2 cm from the center.

For a statistical comparison of this increase between green-spikes and red-spikes zones I normalized the slow-wave/sharp-wave ratio relatively to the values at the center: at 1 cm the increase is 3.5 ± 0.8 and 1.3 ± 0.1 in green-spikes and red-spikes zones, respectively ($P = 0.0007$, Wilcoxon); at 2 cm the increase is of 8.0 ± 2.8 and of 2.6 ± 1.1 in green-spikes and red-spikes zones, respectively ($P = 0.035$, Wilcoxon).

Thus, in green-spikes zones, the discharge waveform differs between center and periphery. In the center, the sharp-wave is tal-

Fig. 1. Green-spikes zones interictal discharges exhibit a peripheral persistence in the slow-wave and in the positive-baseline-shift. **Panel A**. Terminology utilized for the waveforms measured in this study. The prevalent component of an interictal discharge is a sharp-wave followed by a slow-wave. Yet, an interictal discharge most often exhibits a more complex structure, consisting of multiple successive phases with alternating negative and positive polarity. In a subset of the recordings the initial phase was a lower voltage negative phase. Next, in a subset of recordings there was a low voltage positive prepotential that has been previously and extensively described. In this study it was named as the "positive prepotential". Note that established EEG textbooks (Stern and Engel, 2013; Chang et al., 2011) describe the positive prepotential but do not mention a negative polarity phase occurring before that and actually initiating the interictal discharge. Next, the discharge exhibits the typical negative polarity sharp-wave. This is followed by a positive baseline shift and then a slow-wave ensues. The amplitude of each component is measured by the potential difference between its peak and the baseline. Of note, in this study we are arbitrarily naming the initial sharply contoured waveform of IEDs as sharp-waves, independently of their duration, whether shorter or longer than 70 msec. **Panel B** on the left shows data from interictal discharges in foci that do not generate seizures (green spikes). In green-spikes zone, the sharp-wave exhibits a space-dependent decrease in the amplitude: on average it is ~900 μV at the epicenter, and the amplitudes decline down to ~600 μV ($P = 0.002$, Wilcoxon) and ~300 μV ($P = 0.003$, Wilcoxon) at 1 cm and 2 cm, respectively. In the green-spikes zone, the amplitude of the slow-wave remains constant throughout, with values of ~300 μV. The amplitude of the positive-baseline-shift remains constant between center and periphery, too. ** $P < 0.01$, Wilcoxon vs corresponding values of the center. The right side of panel A is a histogram of the ratios positive-baseline-shift/sharp-wave (striped bars) and slow-wave/sharp-wave (empty bars) at the center and at various distances from it. The ratio positive-baseline-shift/sharp-wave is ~0.3 at the center and it increases to ~1.3 at 1 cm ($P = 0.006$, Wilcoxon) and up to 2 at 2 cm ($P = 0.031$, Wilcoxon). At the center, the ratio of slow-wave/sharp-wave is of ~0.7 while it increases to ~1.3 ($P = 0.002$, Wilcoxon) and ~1.8 ($P = 0.02$, Wilcoxon) at distances of 1 cm and 2 cm, respectively. * $P < 0.05$; ** $P < 0.01$, Wilcoxon vs corresponding values of the center. **Panels C** shows voltage traces from intracranial recordings of a green-spikes zone. The traces are average composites. Data are from those electrodes of an 8 × 8 grid that exhibit epileptiform discharges. The location of the traces corresponds to the location of the electrodes whose number is indicated on the side. The trace surrounded by a green dotted line exhibits the highest voltage sharp wave and therefore corresponds to the center of the discharge zone as defined in Methods. The voltage traces show the development of prominent, high voltage, slow-waves (indicated by arrows) in the electrodes surrounding the center. Note that in electrode 36 the amplitude of the discharge is low so that the sharp-and-slow wave morphology cannot be distinguished clearly. Calibration bars are 400 μV and 0.2 sec. The top right panel shows the location of the electrodes' grid. **Panel D** shows data from interictal discharges in foci that generate seizures (red spikes zones). In these, the sharp-wave exhibits a space dependent decrease in the amplitude: on average it is ~800 μV at the epicenter, and the amplitudes decline down to ~500 μV ($P < 0.0001$, Wilcoxon) and ~300 μV ($P = 0.002$, Wilcoxon), at 1 cm and 2 cm, respectively. In the red-spikes zones, the slow-wave exhibits a space-dependent decline that parallels that of the sharp-wave both at 1 cm ($P < 0.0001$, Wilcoxon) and at 2 cm ($P = 0.002$, Wilcoxon). Also, in the red-spikes zones the amplitude of the positive-baseline-shift decays at the periphery in a fashion similar to that of the slow after-wave both at 1 cm ($P < 0.0001$, Wilcoxon) and at 2 cm ($P = 0.002$, Wilcoxon). ** $P < 0.01$ and *** $P < 0.001$, Wilcoxon vs corresponding values of the center. In the histogram over the right of the panel D, the ratio positive-baseline-shift/sharp-wave and slow-wave/sharp-wave remains constant between the center and the periphery of the discharge zone. **Panel E** shows voltage traces from intracranial recordings of a red-spikes zone. The traces are average composites. Data are from those electrodes of an 8 × 8 grid that exhibit epileptiform discharges. The location of the traces corresponds to the location of the electrodes whose number is indicated on the side. The trace surrounded by a red dotted line exhibits the highest voltage sharp-wave and therefore corresponds to the center of the discharge zone as defined in Methods. In the electrodes surrounding the center the amplitude of the sharp-wave declines, but so does the amplitude of the slow-wave. Thus, at 1–2 cm away from the center, discharges appear of lower voltage than at the center, but the relative proportion of the amplitude of the sharp-wave and of the slow-wave remains constant. In contrast, in the green-spikes zone, the peripheral discharges take a different morphology than at the center, exhibiting a prevalence of the slow-wave. Calibration bars are 600 μV and 0.2 sec. The top right panel shows the location of the electrodes' grid.
In sum, green-spikes and red-spikes zones differ in the electrographic morphology of interictal epileptiform discharges. Such difference can be appreciated by comparing waveforms between the center and the periphery of the discharge zone. In the green-spikes zone discharges at the periphery, exhibit lower voltages sharp-waves but maintain robust positive-baseline-shift and slow-waves: the electrographic morphology therefore markedly changes between center and periphery. In contrast, in red-spikes zones, at the periphery the positive-baseline-shift and the slow-wave decay in parallel with the voltage decline of the sharp-wave: a red-spikes zone peripheral discharge has a waveform morphology similar to that of the center, even as the voltage is scaled down. (For interpretation of the references to colour in this figure legend, the reader is referred to the web version of this article.)

Table 2
Green-spikes and red-spikes zones exhibit a subtle, statistically significant difference in the kinetics of the slow-wave.

		Green-spikes zone	Red-spikes zone
Sharp-wave	Ascending phase	72.3 ± 16 μV/msec	117 ± 26 μV/msec
	Descending phase	44.5 ± 12.8 μV/msec	52.6 ± 13.6 μV/msec
	Ascending/Descending	2.1 ± 1.4	3.6 ± 1.1 (*ns*)
	Amplitude/Whole-wave duration	17.6 ± 4.3 μV/msec	13.4 ± 2.9 μV/msec
Slow-wave	Ascending phase	8.2 ± 1.4 μV/msec	8.0 ± 2.0 μV/msec
	Descending phase	2.2 ± 0.8 μV/msec	3.1 ± 0.8 μV/msec
	Ascending/Descending	6.7 ± 1.5	**3.1 ± 0.4***
	Amplitude/Whole-wave duration	1.4 ± 0.4 μV/msec	1.5 ± 0.4 μV/msec

All data are μ ± SE. Note that, that the values of the Ascending/Descending ratios are pure, dimensionless numbers. Differences in the time-course of discharges can be defined quantitatively by measuring the rates (μV/msec) of the ascending and of the descending phases. More *subtle* differences in the waveforms can be identified by calculating the ratios between ascending and descending phases. In addition, the ratio Amplitude/Duration for the whole-wave can provide a quantitative measure of the morphology of the waveform: in discharges with a slower and faster time-course, it would exhibit lower and higher values, respectively. We have performed these measures for both sharp-waves and the slow-waves and compared the corresponding values between green-spikes and red-spikes zones.
Data show that the ascending phase of the sharp-wave is 1.6 ∼ fold steeper in red spikes, though the difference is not statistically significant (*ns*, Wilcoxon). The values of the descending phase, of the ratio ascending/descending and of the ratio Amplitude/Duration for the whole sharp-wave are similar between green-spikes and red-spikes zones. For what concerns the slow-wave, on average, the ascending phase rate, is similar between green-spikes and red-spikes zones. The descending phase rate, however, is steeper in the red-spikes zones and the ratio of Ascending/Descending rates exhibit a statistically significant lower value in the red-spikes zones (* $P = 0.041$, Wilcoxon) consistent with a process decaying more rapidly.
Thus a *novel hypothesis* is: in the red-spikes zones the slow-wave related inhibition is not only lower (Fig. 1), but it also may vanish more rapidly.

ler than the slow-wave, while in the periphery the slow-wave is larger. Relatively to the wording utilized in this study, I am naming this finding as "relative enhancement" or just "increase of the peripheral slow-wave". Differently from the green-spikes zones, at the periphery of red-spikes zones discharges exhibit lower amplitudes but, despite the scaled-down size, the waveform is still similar between center and periphery.

I conclude that the relative enhancement of the peripheral slow-wave correlates with the discharge zone inability to generate seizures.

3.3. Secondary endpoints: positive-baseline-shift is maintained at the periphery in green-spikes zones but is attenuated in red spikes' zones

Pursuing a systematic characterization of all components of IEDs waveforms, I have also measured the voltage of the positive-baseline-shift between the sharp- and the slow-wave. In red-spikes zones, it exhibited a space-dependent decay paralleling that of the sharp-wave. In contrast, in green-spikes zones, it remained constant at increasing distances from the center (Fig. 1B and D, striped bars of the histograms on the left). Thus, in green-spikes zones, the ratio positive-baseline-shift/sharp-wave increases at the periphery of a discharge zone: at the center, this ratio is ∼0.7 while at 1 cm, it increases to 1.3 and at 2 cm, it is ∼2.9. In contrast, in red-spikes zones, it remains constant with values of ∼0.6–0.7 between center and periphery (striped bars of the histograms on the right).

For a statistical comparison between green-spikes and red-spikes zones of this peripheral increase of the positive-baseline-shift/sharp-wave ratio I normalized the positive-baseline-shift/sharp-wave ratio relatively to the values at the center: at 1 cm, the increase is of 1.9 ± 0.3 and 1.1 ± 0.1 in green-spikes and red-spikes zones, respectively ($P = 0.016$, Wilcoxon); at 2 cm, the increase is of 3.2 ± 1.7 and of 1.3 ± 0.4 in green-spikes and red-spikes zones, respectively (ns).

Thus, the increase of the positive-baseline-shift at the periphery, might possibly represent another descriptive feature distinguishing green-spikes and red-spikes zones.

3.4. Secondary end-points: discharges exhibit a low voltage, ***positive*** (downward-going) prepotential of similar amplitudes in green spikes and red spikes

It has long been established that IEDs may commence with a low voltage, positive polarity phase (Chang et al., 2011; Stern and Engel, 2013). In this paper, I am naming this component as the positive prepotential. This component corresponds to EPSPs over deep cortical layers (Pollen, 1964). Thus it may disclose differences on discharges' laminar onset, potentially yielding another marker of the seizure zone.

The positive prepotential was observed in 6/10 of the recordings of the green spikes zone and in 8/16 of the red-spikes zones recordings. I measured the amplitudes in those electrodes where it exhibited the highest voltage: these were 292 ± 96 μV and 255 ± 50 μV for the green-spikes and red-spikes zones, respectively.

Thus, data do not exhibit obvious differences between the green-spikes and red-spikes zones, for this component.

3.5. Secondary end-points: the kinetics of slow-waves but not of sharp waves exhibits a statistically significant difference between green-spikes and red-spikes zones

In brain slices, interictal epileptiform sharp-waves induced by 4-Aminopyridine can assume at least two distinct waveform morphologies. Sharp-waves blocked by bicuculline exhibit longer durations while those blocked by glutamate ionotropic receptor antagonists are faster (De Curtis et al., 2012). I looked for similar differences in discharge kinetics between green-spikes and red-spikes zones.

Data (Table 2) do not show statistically significant differences in the kinetics of sharp-waves between green-spikes and red-spikes zones, though red-spikes zones exhibit a trend (∼1.6 fold) for steeper rise-times. In contrast, slow-waves' kinetics exhibit a subtle, statistically significant difference between green-spikes and red-

Table 3
In both green-spikes and red-spikes zones, the onset lead zone is different from the center and can shift, more often in green-spikes zones.

	Green-spikes zone	Red-spikes zone
Dissociation lead-epicenter	5/10 (50%)	6/16 (37.5%) (*ns*)
Distance lead-epicenter	1.64 ± 0.3 cm	1 ± 0 cm
Shift of lead and spread path	6/10 (60%)	6/16 (37.5%) (*ns*)
Shift (%)	44.7 ± 8.2%	**15.5 ± 5.3%***

Data report values of μ ± SE. In green-spikes zones the dissociation lead-epicenter was more frequent, though this difference was not statistically significant. In green-spikes zones the shift of the spread pathway occurs more frequently than in red-spikes zones. *ns* non-significant with Fisher's exact test $P = 0.689$ for dissociation lead-epicenter and $P = 0.422$ for shift of lead and spread pathway. * $P = 0.045$, Wilcoxon.

spikes zones: in red-spikes zones, the ratio between ascending and descending rates was lower. This preliminary finding may have a plausible explanation: if slow-waves correlate with an inhibitory mechanism, then slow-waves with a more rapid decay, vanishing more rapidly, might possibly facilitate seizures' occurrence.

3.6. Secondary end-points: the cortical surface areas of green-spikes and red-spikes are similar

The IED cortical spatial surface area can be estimated by measuring the number of adjacent electrodes exhibiting discharges: these were 10.3 ± 1.5 and 7.1 ± 0.9 (μ ± SE) in green-spikes and red-spikes zones, respectively. To take into consideration differences in the number of recording electrodes between patients, then, in each patient, I normalized the number of electrodes exhibiting discharges to the number of electrodes of the strip/grid. With this normalization, discharges manifested in 33 ± 9% and in 37 ± 9% of electrodes (μ ± SE) (*ns*) in green-spikes and red-spikes zones, respectively. Thus, there are no differences in the spatial surface area between green-spikes and red-spikes zones.

3.7. Secondary end-points: in the green-spikes zone, discharge onset shifts more frequently

For both green-spikes and red-spikes zones, the electrode exhibiting the highest voltage was consistent throughout consecutive discharges, but was not always the electrode initiating the discharge: there was dissociation between the lead and the center electrodes. Thus, the mechanism of discharges initiation differs from that of hypersynchrony: initiation may require relatively lower hypersynchrony. Rather, hypersynchrony builds up gradually as discharges spread. Such dissociation occurred in both green-spikes and red-spikes zones (Table 3).

The lead electrode was not only different from the center, but also changed throughout the recording: a discharge could initiate from multiple points, transitioning back-and-forth between different spread pathways (Fig. 2): this occurred ~3-fold more frequently in the green-spikes zone (Table 3).

4. Discussion

4.1. Summary of main findings

I found similarities and differences between green-spikes and red-spikes zones that may help to understand ictogenesis. (i) Epileptic discharges morphology differs between center and periphery regarding the slow-waves at the periphery: the latter remain constant in the green-spikes zone but are weakened in the red-spikes zone, and might correspond to surround inhibition. (ii) In the periphery of green-spikes zone the positive-baseline-shift remains robust but is lost in the red-spikes zone. (iii) Slow-wave kinetics shows more rapid decay in the red-spikes zone. (iv) Green-spikes zones exhibit a more frequent shift of the initiators and of propagation pathway.

Green-spikes and red-spikes zones are similar relative to: (i) voltage of the positive prepotential, (ii) sharp-wave kinetics, (iii) spatial surface area.

4.2. Peripheral inhibition: basic mechanism inferences from experimental models applied to human clinical data

More than 50 years ago, surround inhibition was first identified in an animal model of epilepsy (Prince and Wilder, 1967) as a mechanism restraining the spread of cortical epileptiform discharges. Its failure has been thought to result in seizures. Peripheral inhibition has been subsequently observed by several independent investigators (Dichter and Spenser, 1969a, 1969b; Goldensohn and Salazar, 1986; Haglund et al., 1992; Schwartz and Bonhoeffer, 2001).

In neocortical brain slices, salvos of inhibitory synaptic activity restrain focal epileptiform discharges from progressing into seizures (Trevelyan et al., 2006, 2007a, 2007b). In human epilepsy, microelectrodes' recordings have shown that ictal progression corresponds to localized loss of inhibition, too (Schevon et al., 2012).

Microelectrode arrays recordings, though, can be performed only by a few epilepsy centers, are not routinely obtained in surgical evaluations and can sample only a narrow cortical surface. Thus, it is important that the spatial distribution of inhibitory mechanisms may possibly be mapped in routine intracranial EEGs and with technically simple measures, as shown in this paper.

4.3. Peripheral inhibition: basic mechanisms inferences from human clinical data

In routine intracranial EEGs, waveform time-course of epileptiform discharges depends on the underlying basic synaptic and neuronal processes. Thus, a search for features of the EEG wave morphology of epileptiform discharges specific for the red-spikes zone has long been of interest for neurophysiologists as a possible window into basic epilepsy mechanisms. A search for such features (Luders et al., 2006; Palmini, 2006) has been unsuccessful, so far. Thus, this study perhaps might represent the first successful effort to address this question.

The solution of the inverse EEG problem, inferring from macroscopic field potentials of EEG discharges into the locations and strengths of the microscopic generators is not straightforward: different models can explain similar EEG data (Nunez and Srivastava, 2006). Thus, in our study, the inference from epileptiform discharges EEG waveforms into the locations and strength of inhibitory cellular/synaptic mechanism remains just an educated hypothesis.

Yet, other data corroborate the view that epileptic EEG slow-waves reflect inhibitory mechanisms. For example, delta slow-waves correlate with inhibition of the firing rate (Babb and Crandall, 1976; Csercsa et al., 2010) and temporal as well as extratemporal lobe epileptic foci hypometabolism (Henry, 2011; Juhasz and Chugani, 2011) correlates with localized delta slow-waves (Erbayat-Altay et al., 2005; Koutroumadis et al., 2000).

In sum, the data on peripheral slow-wave enhancement support the hypothesis that routine intracranial EEGs might offer a valuable window into a key epilepsy mechanism.

4.4. Positive-baseline-shift may reflect an early inhibitory mechanism

I have also observed that the positive-baseline-shift between the sharp-wave and the slow-wave differs between green-spikes and red-spikes: it exhibits a space-dependent change similar to that of the slow-wave, persisting from the center into the periphery of green spikes. Cellular/synaptic correlates of the positive-baseline-shift have been studied less than those of the slow wave. The positive polarity indicates dipole's direction from-deep-to-superficial layers: this can result from a deep laminae sink and/or from a superficial laminae source (such as early superficial repolarization/hyperpolarization). In the latter case, it might represent an early inhibitory process, thus, with a time-course matching experimental models' fast inhibitory afterpotentials (Witte, 1994).

4.5. Green spikes zones exhibit more frequent shifts of the initiating electrodes

I observed that green-spikes zones exhibited more frequent shifts in the spread pathway. Shifting initiators have been observed

also in IEDs of brain slices, (Trevelyan et al., 2007a; Serafini et al., 2015, 2016) and in human neocortex (Trevelyan et al., 2007a): an epileptic discharge region is likely composed of multiple distinct generators, each capable of independent activity, and yet interconnected. Microfoci have been observed in non-epileptic cortex (Stead et al., 2010): the progression from normal into chronic epileptic cortex might reflect the multiplication and interconnection of such small scale domains of epileptic hyperexcitability

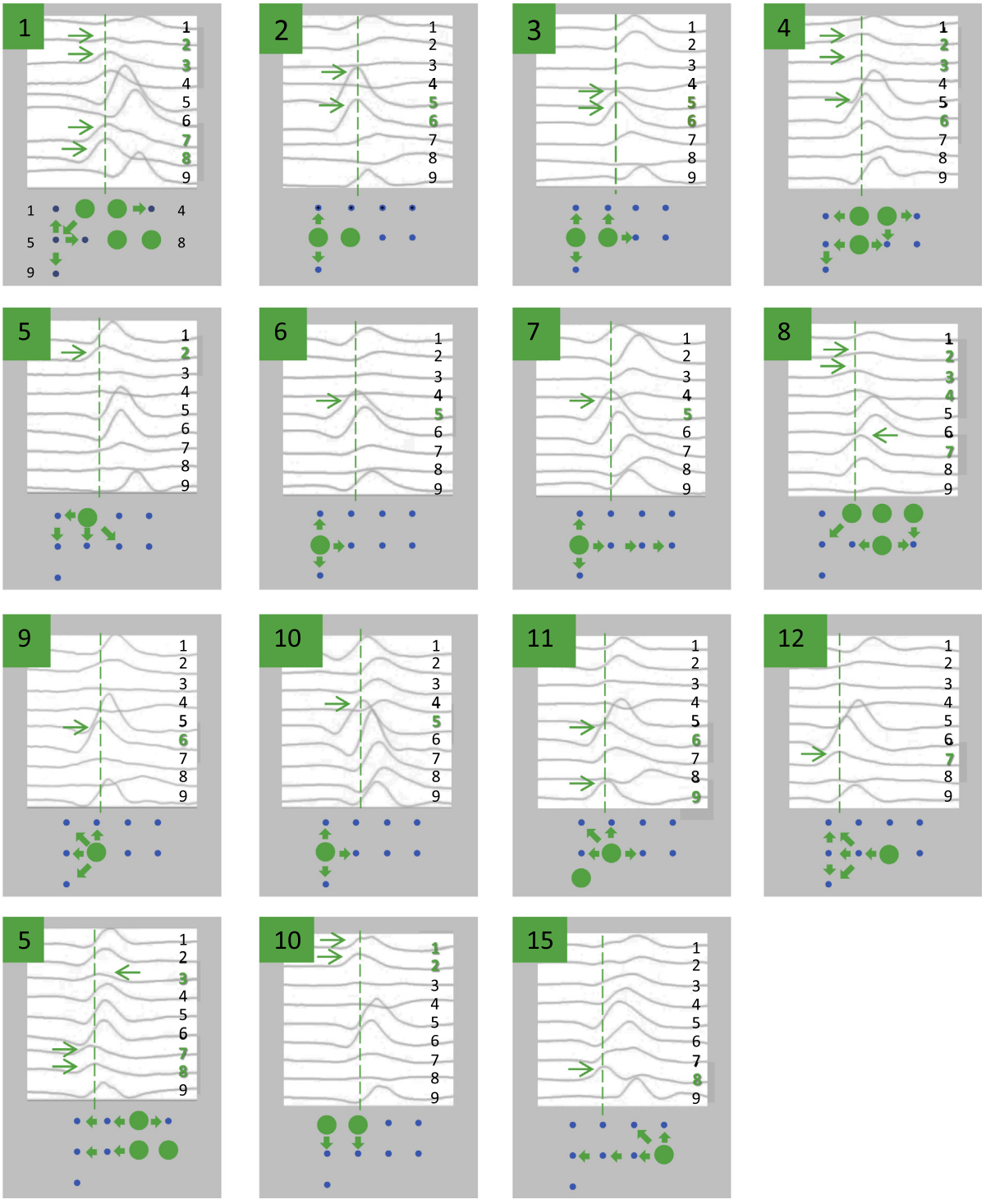

(Serafini et al., 2015, 2016). The decrease in back-and-forth shift of initiators and spread pathway suggests, hypothetically, a distinct evolution for epileptogenic zones: the ability to generate seizures might occur only after a preferential spread pathway prevails.

5. Limitations of the study

This study has at least three main limitations.

First, this study averaged the values of waveforms in different points along the spread zone. Yet, peripheral slow-wave persistence may vary in different sectors of the perimeter and inhibitory cortical regions may be distributed in a mosaic, patchy, mottled fashion (discussed in Engel, 1990) rather than surrounding a discreet focus. It is also possible, that prolonged recordings may exhibit variations in time of the peripheral slow-wave persistence. A characterization of these aspects would require more data, with longer recordings and a larger number of patients' cases.

Second, as shown in Table 1, the pathologies underlying the discharge zone varied considerably. This study averaged data from patients with a breath of conditions. But different pathologies may generate discharge zones with distinct neurophysiological properties. This study is, however, underpowered to offer even only hypotheses on this matter.

Finally, a third limitation is the absence of single unit recordings in the study: the correspondence between the slow-wave and neurophysiological inhibition has long and broadly been assumed in the epilepsy neurophysiology literature and, accordingly, was assumed, in this manuscript, too.

These are important and complex issues. They could not be addressed *yet*, in this paper and they deserve a dedicated and extended focus, beyond the initial scope of our study.

6. Summary and conclusions

IEDs' morphology exhibits a spatial organization with a *peripheral* prevalence or relative increase of the slow-wave. Such center-vs-periphery difference is pronounced in green-spikes zones and, vice-versa is attenuated in red-spikes zones. Thus, peripheral slow-waves' relative enhancement may correspond to surround inhibition. Additional green-spikes zones' features are a positive-baseline-shift persisting from the center into the periphery, slow-wave kinetics with relatively slower decays, and an increase in the back-and-forth shift of spread pathways.

To the old question of how to distinguish green-spikes from red-spikes zones, this study offers a novel and technically simple approach: waveform analysis of interictal discharges of intracranial EEGs may potentially offer a window on ictogenesis mechanism, and also be integrated with imaging studies to identify seizures' zones.

Acknowledgements

Orhan Bican, Noel Carlson, Jeff Loeb, Biswajit Marathi, Fred Matsuo and John Rolston have provided important and constructive critiques to an initial version this paper.

This study was supported by a start-up fund provided to the author by the Department of Neurology of the University of Utah.

Conflict of interest

Nothing to report.

References

Babb TL, Crandall PH. Epileptogenesis of human limbic neurons in psychomotor epileptics. Electroencephalogr Clin Neurophysiol 1976;40:225–43.
Buzsáki G. Hippocampal sharp waves: their origin and significance. Brain Res 1986;398:242–52.
Chang BS, Schomer DL, Niedermeyer E. Epilepsy in adults and the elderly. In: Niedermeyer E, Lopes Da Silva FH, editors. Niedermeyer's electroencephalography: basic principles. 6th ed. Wolters Kluwer; 2011. p. 1018–25.
Csercsa R, Dombovari B, Fabo D, Wittner L, Eross L, Entz L, et al. Laminar analysis of slow wave activity in human brain. Brain 2010;133:2814–28.
De Curtis M, Jefferys JGR, Avoli M. Interictal epileptiform discharges in partial epilepsy: complex neurobiological mechanisms based on experimental and clinical evidence. In: Noebels JL, Avoli M, Rogawski MA, Olsen RW, Delgado-Escueta AV, editors. Jasper's basic mechanisms of the epilepsies. Oxford University Press; 2012. p. 303–326. Internet edition at: http://www.ncbi.nlm.nih.gov/books/NBK98179/pdf/decurtis.pdf.
Dichter M, Spencer WA. Penicillin-induced interictal discharges from the cat hippocampus. I. Characteristics and topographical features. J Neurophysiol 1969a;32:649–62.
Dichter M, Spencer WA. Penicillin-induced interictal discharges from the cat hippocampus. II. Mechanisms underlying origin and restriction. J Neurophysiol 1969b;32:663–87.
Engel J. Functional explorations of the human epileptic brain and their therapeutic implications. Electroencephalogr Clin Neurophysiol 1990;76:296–316.
Erbayat-Altay EA, Fessler AJ, Gallagher M, Attarian HP, Dehdashti F, Vahle VJ, et al. Correlation of severity of FDG-PET hypometabolism and interictal regional delta slowing in temporal lobe epilepsy. Epilepsia 2005;46:573–6.
Goldensohn ES, Salazar AM. Temporal and spatial distribution of intracellular potentials during generation and spread of epileptogenic discharges. Adv Neurol 1986;44:559–82.
Haglund MM, Ojemann GA, Hochman DW. Optical imaging of epileptiform and functional activity in human cerebral cortex. Nature 1992;358:668–71.
Henry T. Positron Emission tomography: glucose metabolism studies in temporal lobe epilepsy. In: Chugani HT, editor. Neuroimaging in epilepsy. Oxford University Press; 2011. p. 122–40.
Jehi L. Mesial temporal lobectomy: post-surgical seizure frequency. In: Luders HO, editor. Textbook of epilepsy surgery. Informa UK; 2008. p. 1223–35.
Juhasz C, Chugani HT. Positron emission tomography: glucose metabolism in extratemporal lobe epilepsy. In: Chugani HT, editor. Neuroimaging in epilepsy. Oxford University Press; 2011. p. 141–55.
Koutroumadis MM, Binnie CD, Elwes RS, Polkey CE, Seed P, Alarcon G, et al. Interictal regional slow activity in temporal lobe epilepsy correlates with lateral temporal hypometabolism as imaged with ^{18}FDG PET: neurophysiological and metabolic implications. J Neurol Neurosurg Psychiatry 2000;65:170–6.
Luders HO, Najm I, Nair D, Widdess-Walsh P, Bingman W. The epileptogenic zone: general principles. Epileptic Disord 2006;8(Suppl 2):S1–9.
Matsumoto H, Ajmone-Marsan C. Cortical cellular phenomena in experimental epilepsy: interictal manifestations. Exp Neurol 1964;9:286–304.
Noe K, Sulc V, Wong-Kisiel L, Wirrell E, Van Gompel JJ, Wetjen N, et al. Long-term outcomes after non-lesional extratemporal lobe epilepsy surgery. JAMA Neurol 2013;70:1003–8.
Nunez PL, Srivastava R. Fallacies in EEG 2006. In: Nunez PL, Srivastava R, editors. Electric fields of the brain. The neurophysics of EEG. Oxford University Press; 2006. p. 56–98.
Palmini A. The concept of the epileptogenic zone: a modern look at Penfield and Jasper's views on the role of interictal spikes. Epileptic Disord 2006;8(Suppl 2):S10–5.
Pollen DA. Intracellular studies of cortical neurons during thalamic induced wave and spike. Electroencephalogr Clin Neurophysiol 1964;17:398–406.
Prince D, Wilder BJ. Control mechanisms in control epileptogenic foci. Arch Neurol 1967;16:194–202.

Fig. 2. Human interictal epileptiform discharges initiate from multiple points. The figure shows voltage traces from fifteen consecutive discharges recorded from an intracranial grid of a patient with intractable epilepsy. The data were recorded from an 8 × 8 subdural grid of electrodes. Each panel corresponds to a discharge event. For the sake of simplification or clarity, the data shown in each upper panel are from a selection of nine adjacent electrodes exhibiting discharges and we are not showing traces from electrodes without discharges. Vertical lines represent the leads where discharges originate. The bottom of each panel represents the 9 electrodes from which traces are recorded. Each electrode corresponds to a small circle. Large circles represent electrodes in which discharges arise corresponding to the vertical lines of the upper panels. Arrows indicate the pathways and directions in the locations where discharges spread to the adjacent zones. Calibration bars are 1000 μV and 0.1 sec. The data show a constant change in the lead electrodes and in the corresponding pathways/directions of spread in each subsequent discharge event. A discharge zone may therefore be composed my multiple interconnected small domains that can fire independently from one another. Each of them, can, in its own turn, initiate the discharge event spreading to the adjacent ones.

Schevon CA, Weiss SA, McKhann G, Goodman RR, Yuste R, Emerson RG, et al. Evidence of an inhibitory restraint of seizure activity in humans. Nat Commun 2012;3:1060.
Schwartz TH, Bonhoeffer T. In vivo optical mapping of epileptic foci and surround inhibition in ferret cerebral cortex. Nat Med 2001;7:1063–7.
Serafini R, Loeb JA. Enhanced slow waves at the periphery of human epileptic foci. Clin Neurophysiol 2015;126:1117–23.
Serafini R, Andrade R, Loeb JA. Coalescence of deep and superficial epileptic foci into larger discharge units in adult rat neocortex. Neuroscience 2015;292:148–58.
Serafini R, Dettloff S, Loeb JA. Neocortical slices from adult chronic epileptic rats exhibit discharges of higher voltages and broader spread. Neuroscience 2016;322:509–24.
Stead M, Bower M, Brinkman BH, Lee K, Marsch WR, Meyer FB, et al. Microseizures and the spatiotemporal scales of human partial epilepsy. Brain 2010;133:2789–97.
Stern JM, Engel JE. Interictal epileptiform patterns. In: Stern JM, Engel JE, editors. Atlas of EEG patterns. 2nd ed. Lippincott Williams & Wilkins; 2013. p. 249–80.
Trevelyan AJ, Sussillo D, Watson BO, Yuste R. Modular propagation of epileptiform activity: evidence for an inhibitory veto in neocortex. J Neurosci 2006;26:12447–55.
Trevelyan AJ, Baldeweg T, van Drongelen W, Yuste R, Whittington M. The source of after-discharge activity in neocortical tonic-clonic epilepsy. J Neurosci 2007a;27:13513–9.
Trevelyan AJ, Sussillo D, Yuste R. Feedforward inhibition contributes to the control of epileptiform propagation speed. J Neurosci 2007b;27:3383–7.
Trevelyan AJ, Schevon CA. How inhibition influences seizure propagation. Neuropharmacology 2012;69:45–54.
Witte OW. Afterpotentials of penicillin-induced epileptiform neuronal discharges in the motor cortex of the rat in vivo. Epilepsy res 1994;18:43–55.